Received: 9 December 2016

DOI: 10.1002/mop.30597

Wideband bandstop filter using spurline and symmetric coupled open stubs

Hyun-Seung Lee[1] | Jeong-Taek Lim[1] | Bang-Chul Jung[1] | Jong-Myung Woo[2] | Choul-Young Kim[1]

[1] Department of Electronics Engineering, Chungnam National University, Republic of Korea

[2] Department of Radio and Information Communications Engineering, Chungnam National University, Republic of Korea

Correspondence
Choul-Young Kim, Department of Electronics Engineering, Chungnam National University, Republic of Korea.
Email: cykim@cnu.ac.kr

Funding information
National Research Foundation of Korea (NRF), Grant Number: NRF–2016R1A2B4014834

Abstract
In this article, we propose a structure that can extend the stopband of the bandstop filter (BSF). The bandwidth of the BSF can be extended by symmetrically combining the BSFs that electrically couple the ends of two open stubs located in parallel on a single microstrip transmission line containing a spurline. The bandwidth of the stopband of the BSF proposed in this article is increased to 3.5 GHz. We confirm that when compared to parallel open stubs without spurline filters, the stopband bandwidth is extended by approximately 289% (rejection depth: −20 dB).

KEYWORDS
bandstop filter, coupling, spurline, open stub, wideband

1 | INTRODUCTION

A conventional bandstop filter (BSF) can be designed using only a parallel open microstrip stub; the plate spurline grooves in the microstrip line form the BSF.[1–3] However, the drawback of this kind of filter is that it has a very narrow stopband. This problem can be solved in several ways: by inserting several open stubs in parallel, spaced $\lambda/4$ apart; or by combining open stubs with spurlines.[4,5] However, these methods cannot extend the bandwidth effectively. To overcome these issues, electrically coupled open stub (ECOS) BSFs have been developed recently (Figure 1C,D) to control the stopband of the filter by adjusting the gap and lengths of the two open stubs.[6] In this article, we were able to extend the bandwidth of a BSF by symmetrically combining the BSFs that electrically couple the ends of two open stubs located in parallel on a single microstrip transmission line containing a spurline. Figure 2 shows the structure of the proposed wideband compact BSF designed to extend the stopband bandwidth.

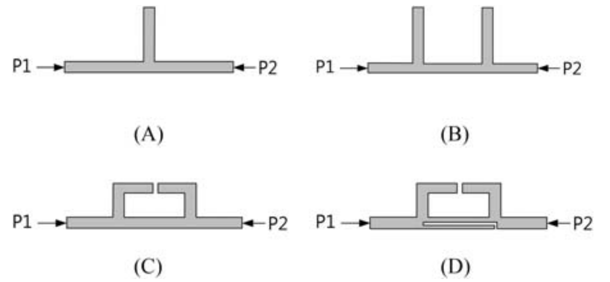

FIGURE 1 BSFs using open stubs and spurline[4]: (A) open stub filter, (B) shunt quarter-wavelength open stub filter, (C) electrically coupled open stub (ECOS) filter, and (D) ECOS filter with spurline

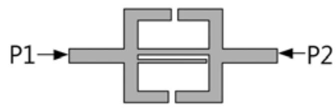

FIGURE 2 Proposed structure of BSF with spurline and symmetric ECOS BSFs

2 | DESIGN AND FABRICATION

The details of the proposed BSF are shown in Figure 3. The gap between the ends of the open stubs is 0.4 mm, and the spacing of spurline is 0.34 mm. The width of the open stub is 1.7 mm, and its length is 9.8 mm. Table 1 shows the parameters of the proposed BSF.

Figure 4 shows the schematic of the proposed BSF. It can be divided into three parts: U, S, and B. The Y parameters of the entire BSF are given by

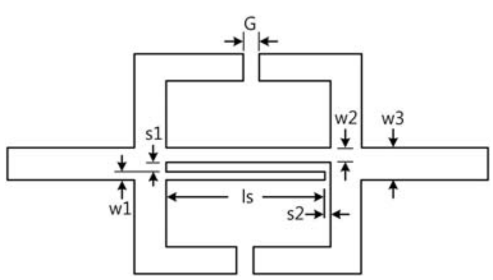

FIGURE 3 Configurations of the designed BSF

TABLE 1 Parameters of the proposed BSF

Parameter	Value [mm]
G	0.4
w1	0.34
w2	1.02
w3	1.7
s1	0.34
s2	0.34
Ls	9.66

$$\begin{bmatrix} Y_{11,T} & Y_{12,T} \\ Y_{21,T} & Y_{22,T} \end{bmatrix} = \begin{bmatrix} Y_{11,U} & Y_{12,U} \\ Y_{21,U} & Y_{22,U} \end{bmatrix} + \begin{bmatrix} Y_{11,S} & Y_{12,S} \\ Y_{21,S} & Y_{22,S} \end{bmatrix} + \begin{bmatrix} Y_{11,B} & Y_{12,B} \\ Y_{21,B} & Y_{22,B} \end{bmatrix} \quad (1)$$

where the first part, related to the U, can be calculated from the following equations.

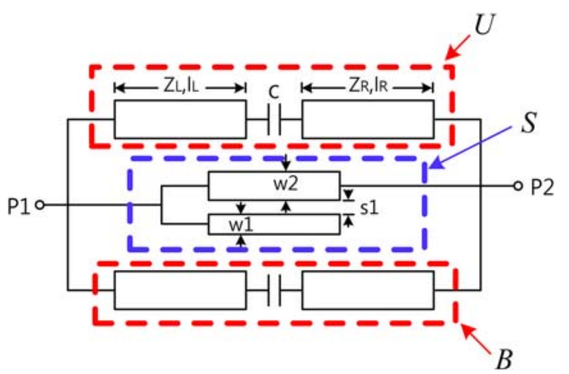

FIGURE 4 Schematic of the proposed BSF. [Color figure can be viewed at wileyonlinelibrary.com]

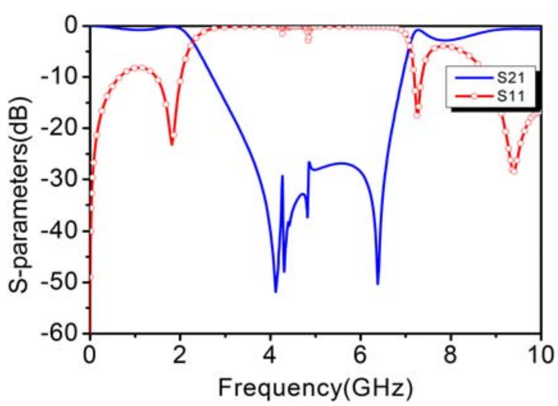

FIGURE 5 S-parameters of the proposed BSF (simulation). [Color figure can be viewed at wileyonlinelibrary.com]

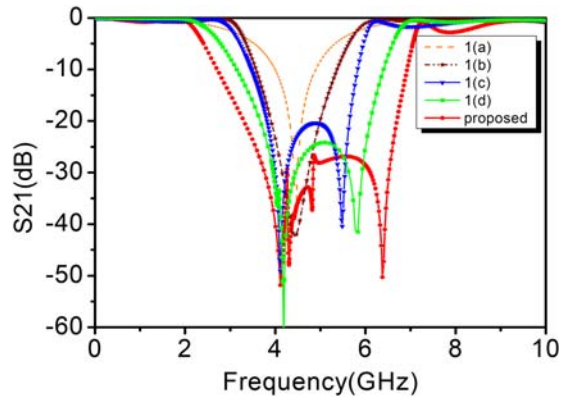

FIGURE 6 Comparison of S_{21}s of BSFs (simulation). [Color figure can be viewed at wileyonlinelibrary.com]

$$\begin{bmatrix} Y_{11,U} & Y_{12,U} \\ Y_{21,U} & Y_{22,U} \end{bmatrix} = \begin{bmatrix} \frac{D_U}{B_U} & \frac{B_U C_U - A_U D_U}{B_U} \\ \frac{-1}{B_U} & \frac{A_U}{B_U} \end{bmatrix} \quad (2)$$

$$\begin{bmatrix} A_U & B_U \\ C_U & D_U \end{bmatrix} = \begin{bmatrix} A_L & B_L \\ C_L & D_L \end{bmatrix} \begin{bmatrix} A_C & B_C \\ C_C & D_C \end{bmatrix} \begin{bmatrix} A_R & B_R \\ C_R & D_R \end{bmatrix}$$

$$= \begin{bmatrix} -\sin\theta & jZ_0\cos\theta \\ jY_0\cos\theta & -\sin\theta \end{bmatrix} \begin{bmatrix} 1 & -j\frac{Z_0}{\left(1+\frac{2}{\pi}\theta\right)b_c} \\ 0 & 1 \end{bmatrix} \begin{bmatrix} -\sin\theta & jZ_0\cos\theta \\ jY_0\cos\theta & -\sin\theta \end{bmatrix}$$

where $\theta = \frac{\pi}{2}\frac{f-f_0}{f_0}$, $l_L = l_R = l_B = \frac{\lambda_0}{4}$,

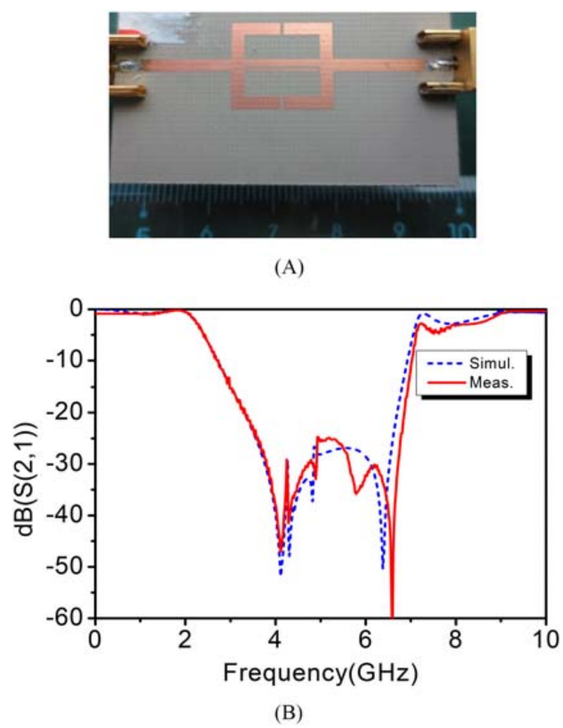

FIGURE 7 (A) Photograph of the fabricated symmetric ECOS BSF, (B) S-parameters (S_{21}). [Color figure can be viewed at wileyonlinelibrary.com]

TABLE 2 Comparison of the stopband, stopband bandwidth, and increasing rate of stopband bandwidth

BSF	Stopband (rejection depth: −20 dB) [GHz]	Stopband bandwidth [GHz]	Increasing rate of stopband bandwidth [%]
(a) Open stub	4.4~4.6	0.2	−78
(b) Dual open stubs	4.0~4.9	0.9	0 (Reference)
(c) ECOS	4.0~5.5	1.5	67
(d) ECOS & spurline	3.9~6.0	2.1	133
(e) ECOS & symmetric dual spurline	3.3~6.8	3.5	289

$$B_c=\omega C=\left(1+\frac{2}{\pi}\theta\right)b_cY_0,\quad b_c=(2\pi f_0C)Z_0.$$

The second part, related to the S (spurline), is derived from the following equations.[7–9]

$$\begin{bmatrix} Y_{11,S} & Y_{12,S} \\ Y_{21,S} & Y_{22,S} \end{bmatrix}=\begin{bmatrix} \frac{D_S}{B_S} & \frac{B_SC_S-A_SD_S}{B_S} \\ \frac{-1}{B_S} & \frac{A_S}{B_S} \end{bmatrix} \tag{3}$$

$$A_s=\frac{\cos\theta_C\cos\theta_\pi(R_C-R_\pi)}{R_C(1-R_\pi)\cos\theta_\pi-R_\pi(1-R_C)\cos\theta_C}$$

$$C_s=\frac{j}{R_C(1-R_\pi)\cos\theta_\pi-R_\pi(1-R_C)\cos\theta_C}$$

$$\left[\frac{(1-R_C)^2\cos\theta_C}{R_CZ_{01\pi}\csc\theta_\pi}-\frac{(1-R_\pi)^2\cos\theta_\pi}{R_\pi Z_{01C}\csc\theta_C}\right]$$

$$D_s=\left\{\begin{array}{c} cos\theta_C cos\theta_\pi\left[R_\pi^2(1-R_C)^2+R_C^2(1-R_\pi)^2\right] \\ +R_CR_\pi sin\theta_C sin\theta_\pi \\ \cdot\left[\frac{Z_{01C}}{Z_{01\pi}}(1-R_C)^2+\frac{Z_{01\pi}}{Z_{01C}}(1-R_\pi)^2\right] \\ -2R_CR_\pi(1-R_C)(1-R_\pi) \end{array}\right\}$$

$$/(R_C-R_\pi)[R_C(1-R_\pi)\cos\theta_\pi-R_\pi(1-R_C)\cos\theta_C]$$

and

$$B_s=\frac{1}{C}(AD-1)$$

where $\theta_{C,\pi}$ represents the electrical lengths of the line for the two modes (C, π.), $R_C=1$,

$$R_\pi=-(C_1-C_{12})/(C_2-C_{12}),$$

$$Z_{01k}=\frac{1}{v_k(C_{11}+R_kC_{12})}=\frac{1}{Y_{01k}},\quad(k=c,\pi)$$

The third part, related to B, is derived by

$$\begin{bmatrix} Y_{11,B} & Y_{12,B} \\ Y_{21,B} & Y_{22,B} \end{bmatrix}=\begin{bmatrix} Y_{11,U} & Y_{12,U} \\ Y_{21,U} & Y_{22,U} \end{bmatrix} \tag{4}$$

Figure 5 shows the simulated S parameters. From the simulation, the stopband bandwidth is obtained as 3.36 GHz (rejection depth: −20 dB, 3.33–6.69 GHz). Figure 6 shows the comparison between the S_{21} of the proposed ECOS BSF and that of the existing BSFs. We confirmed that, compared to the parallel open stubs without spurline filters (Figure 1B), the stopband bandwidth was extended by approximately 214% (rejection depth: −20 dB).

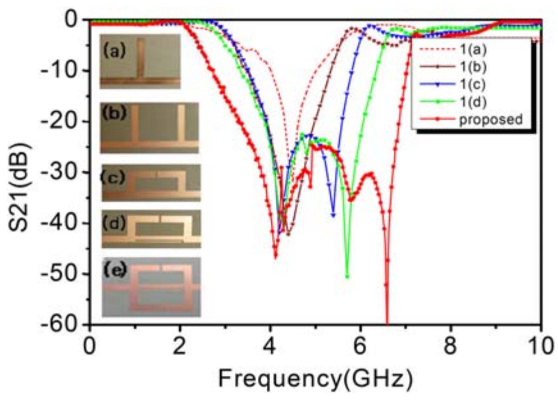

FIGURE 8 Comparison of S_{21}s of BSFs (measured). [Color figure can be viewed at wileyonlinelibrary.com]

3 | MEASUREMENT RESULTS

Based on the simulation results, the proposed BSF was fabricated on an RF-35 substrate (thickness 30 mil). Agilent's 8719ES vector network analyzer was used to measure the fabricated BSF. A photograph of the fabricated BSF is shown in Figure 7A. Figure 7B shows the simulated and measured results from the proposed filter. Figure 8 shows the comparison of the insertion losses of conventional BSFs ((a)–(d)) and that of the filter proposed in this article ((e)). The stopband of the proposed filter ((e)) is extended to 3.3 GHz (3.3–6.8 GHz) and increased by approximately 289% (rejection depth: −20 dB) compared to the case in which the dual spurline ((b)) is not combined. Table 2 shows the comparison of the stopband, stopband bandwidth, and increasing rate of stopband bandwidth.

4 | CONCLUSION

In this article, the stopband bandwidth of a BSF was significantly extended by symmetrically combining the two ECOS BSFs, which electrically coupled the ends of two open stubs located in parallel on a single microstrip transmission line containing a spurline. The stopband bandwidth of the BSF proposed in this article is increased to 3.5GHz. We confirmed that compared to the parallel open stubs without the spurline filter, stopband bandwidth was extended to the approximately 289% (rejection depth: −20dB).

ACKNOWLEDGMENTS

This research supported by the Basic Science Research Program through the National Research Foundation of Korea (NRF) funded by the Ministry of Science, ICT & Future Planning (MSIP) (NRF–2016R1A2B4014834).

REFERENCES

[1] Hong JS, Lancaster MJ. *Microstrip Filters for RF/Microwave Applications*. New York: John Wiley; 2001.

[2] Gorur A, Karpuz C. Uniplanar compact wideband bandstop filter. *IEEE Microwave Wireless Compon Lett* 2003;13:114–116.

[3] Hsieh MY, Wang SM. Compact and wideband microstrip bandstop filter. *IEEE Microwave Wireless Compon Lett* 2005;15:472–474.

[4] Tu WH, Chang K. Compact microstrip bandstop filter using open stub and spurline. *IEEE Microwave Wireless Compon. Lett* 2005; 15:268–270.

[5] Mandal MK, Sanyal S. Compact bandstop filter using signal interference technique. *IET Electron Lett* 2007;43:110–111.

[6] Lee HS, Lim WG, Kim CY. Compact wideband bandstop filters with electrically coupled open stubs. *Microwave Opt Technol Lett* 2013;55:2701–2703.

[7] Allen JL. Non-symmetrical coupled lines in an inhomogeneous dielectric medium. *Int J Electron* 1975;38:337–347.

[8] Tripathi VK. Equivalent circuits and characteristics of inhomogeneous nonsymmetrical coupled-line two-port circuits. *IEEE Trans Microwave Theory Tech* 1977;25:140–142.

[9] Nguyen C, Chang K. On the analysis and design of spurline bandstop filters. *IEEE Trans Microwave Theory Tech* 1985;33:1416–1421.

How to cite this article: Lee H-S, Lim J-T, Jung B-C, Woo J-M, Kim C-Y. Wideband bandstop filter using spurline and symmetric coupled open stubs. *Microw Opt Technol Lett.* 2017;59:1605–1608. https://doi.org/10.1002/mop.30597

Received: 10 December 2016

DOI: 10.1002/mop.30596

A pattern-reconfigurable water-loaded MIMO antenna

Ya-Hui Qian | Qing-Xin Chu

School of Electronic and Information Engineering, South China University of Technology, Guangzhou, Guangdong, People's Republic of China

Correspondence
Qing-Xin Chu, School of Electronic and Information Engineering, South China University of Technology, Guangzhou, Guangdong, People's Republic of China.
Email: qxchu@scut.edu.cn

Abstract

A novel radiation pattern reconfigurable multiple-input multiple-output (MIMO) antenna based on the loading of water is presented. By altering the situation of loading and unloading the distilled water on the surface of the parasitic element, the function of the parasitic element can be switched between a director and a reflector. According to the Yagi-Uda principle, the antenna creates a directional radiation pattern in the azimuth plane through the electromagnetically coupled parasitic elements. A good direction is achieved with the front-to-back of 13 dBi. The MIMO antenna consists of 2 identical elements lying orthogonally to each other. As a result, high-isolation (>35 dB) and low-envelop correlation coefficient ($\rho_e < 0.0001$) between MIMO elements are obtained by orthogonal dual-polarization antenna element. Good agreement is achieved between the measured results and the simulated results.

KEYWORDS

dual polarization, multiple input multiple output (MIMO) antenna, pattern reconfiguration, water, Yagi-Uda antenna

1 | INTRODUCTION

Pattern reconfigurable antennas providing the ability to dynamically alter their radiation patterns have drawn considerable attention; they are useful for modern wireless communication systems which have different requirements in the last decade. With manipulation of the radiation pattern of antenna, the quality and security of the communication can be improved, as the noise source can be avoided and the